Time to change your mind? Modelling transient properties of cortex formation highlights the importance of evolving cell division strategies

Noemi Picco*

University of Oxford, Mathematical Institute, Woodstock Road, Oxford, OX2 6GG.

Thomas E. Woolley

Cardiff School of Mathematics, Cardiff University, Senghennydd Road, Cardiff, CF24 4AG

August 12, 2018

Abstract

The successful development of the mammalian cerebral neocortex is linked to numerous cognitive functions such as language, voluntary movement, and episodic memory. Neocortex development occurs when neural progenitor cells divide and produce neurons. Critically, although the progenitor cells are able to self-renew they do not reproduce themselves endlessly. Hence, to fully understand the development of the neocortex we are faced with the challenge of understanding temporal changes in cell division strategy. Our approach to modelling neuronal production uses non-autonomous ordinary differential equations and allows us to use a ternary coordinate system in order to define a strategy space, through which we can visualise evolving cell division strategies. Using this strategy space, we fit the known data and use approximate Bayesian computation to predict the founding progenitor population sizes, currently unavailable in the experimental literature. Counter-intuitively, we show that humans can generate a larger number of neurons than a macaque's even when starting with a smaller number of progenitor cells. Accompanying the article is a self-contained piece of software, which provides the reader with immediate simulated results that will aid their intuition. The software can be found at www.dpag.ox.ac.uk/team/noemi-picco.

1 Introduction

Biological systems are hardly ever stationary. Indeed, as Alan Turing once said "Most of an organism, most of the time, is developing from one pattern into another [...]. One would like to be able to follow this more general process mathematically also. The difficulties are, however, such that one cannot hope to have any very embracing theory of such processes, beyond the statement of the equations" [1]. Although mathematical techniques for detecting, interrogating and simulating transient dynamical system have been developed in the following years [2–8] it is still standard for mathematical biologists to use autonomous equations and consider only the stable stationary states of their models as defining the developmental outcomes of biological systems.

Here, we model the development of the mammalian cerebral neocortex, which is a highly dynamic and an incredibly important biological system. The development of a fully functioning cortex is linked

*picco@maths.ox.ac.uk

to numerous cognitive functions such as language, voluntary movement, and episodic memory [9]. Conversely, pathological development can lead to diseases, such as microcephaly [10].

The neocortex is comprised of neurons produced by neural progenitor cells [11]. Critically, although the progenitor cells are able to self-renew (like their parent neuroepithelial stem cells) they do not reproduce themselves endlessly. Specifically, they undergo a shift in division strategy. Early in the development of the neocortex the progenitor cell populations are maintained through symmetric and asymmetric divisions, which produce either two progenitor cells, or a progenitor and a neuron. Later in development progenitor cell reproduction drops dramatically with neuronal production becoming dominant. Note that some progenitor self renewal will still occur, as these cells will go on to accomplish gliogenesis [12]. Hence, to fully understand the development of the neocortex we are faced with the challenge of fundamentally understanding the temporal changes in cell division strategy.

Beyond the core problem described above the development of a normal cortex is further complicated by many factors, such as [11, 13, 14]:

- the size of the founder population present at the beginning of cortical neurogenesis;
- neurogenesis duration;
- cell cycle dynamics;
- cell migration into the developing cortex;
- programmed cell death;
- the balance between self-renewing and differentiative divisions.

Variations in any one of these factors generally leads to an intuitive change in the resulting neuronal number, which in the following will be referred to as *neurogenic output*. For example prolonging the time devoted to amplification of the founder population results in expanded neuronal number [15]. However, biological development is more than the sum of its parts and, thus, we have to provide a mechanism that specifies how combinations of such factors work together to ensure the cortex is correctly formed.

Quantitative data specifying the cellular populations of the cortex, are beginning to appear [16]. However, these studies do not, as yet, provide an underlying mechanism explaining transitions in cellular identity, as they focus preferentially on providing scaling rules that explain the correlations between neurogenic output and factors such as brain volume and length of neurogenesis [17].

As a means of offering mechanistic insights even in the face of missing data we develop a theoretical model of progenitor cell proliferation and neuronal production. Critically, it is suggested that there are already over 150 different mathematical models [18] of the cell cycle spanning multiple different cell types, such as frog eggs [19] and drosophila [20]. Equally, the mathematical approaches to modelling differentiation dynamics range over many fields, such as stochastic models [21], time delays [22] and Boolean logic [23]. Critically, nearly all of the suggested models deal with understanding small, often hypothetical, parts of the cycle rather than the evolution of the population size. Of the neuro developmental models that do consider neuron population production they are usually focussed on different parts of the brain (which requires different assumptions), do not include the observed time dependent evolution of the cellular division strategy, or are involved with different dynamical states (e.g. homeostasis) [24–26].

Our approach matches closest to that seen in the work on cerebellum development [27]. Namely, we use non-autonomous ordinary differential equations (ODEs) to capture the change in progenitor cell division strategy over time during cortex development of the species of interest [28].

Since available quantitative data is minimal our model is a parsimonious representation of a minimal set of processes and players providing a general, yet accurate, mechanism of cortical neurogenesis. Our most counter-intuitive result is that a larger cortex does not necessarily derive from a larger initial population of progenitor cells. Specifically, we show that, under the current assumptions on cell cycle

dynamics, humans can generate more neurons than macaques and mice even when starting with a smaller number of progenitor cells.

The paper is structured as follows, we construct a non-autonomous ODE model of progenitor proliferation and differentiation and use a ternary coordinate system to define a strategy space, through which we can visualise the transient behaviour of cell differentiation. Having created the framework we search the strategy space to find the strategy, or strategies, matching the observed patterns of neurogenic output of the mouse, macaque and human. From this point, we use approximate Bayesian computation to predict the founding progenitor population sizes, currently unavailable in the experimental literature. This is achieved via fit of the species-specific model to experimentally obtained final neuron population sizes.

A graphical user interface (GUI) solving the presented ODE system accompanies this paper. This provides the biological reader with immediate simulated results that can aid their intuition as to how cortex development will progress in perturbed scenarios. Equally, the interested reader is able to rapidly investigate the sensitivity of our results to their additional knowledge and data. Further, where sensitivity occurs and data is lacking then we are able to direct future biological experimental efforts through gaining the missing data and, as such, test our hypotheses. The neurogenesis simulator is available for download at www.dpag.ox.ac.uk/team/noemi-picco.

2 Mathematical model of cell differentiation

We aim to construct a minimal dynamic model linking an initial population of progenitor stem cells, P, (which is able to reproduce itself) to a finally differentiated, post-mitotic neuron population, N. We consider three possible modes of progenitor cell division: self-amplifying (symmetric) division, D_s, which generates two identical progenitors; asymmetric neuronal division, D_a, generating one progenitor and one neuron; symmetric neuronal division, D_n, generating two neurons (see Figure 1).

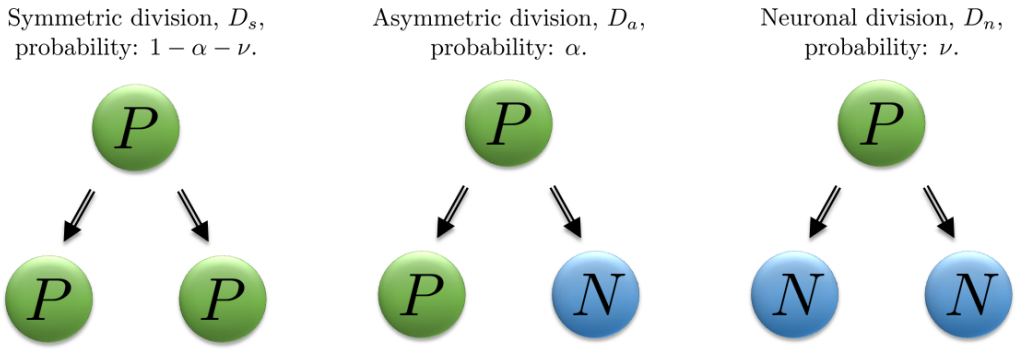

Figure 1: Schematic diagram illustrating the three types of cellular division, from progenitor, P, to other progenitors and/or neurons, N. The transition probabilities, α, ν and $1-\alpha-\nu$ are also illustrated.

The progenitor population includes all pre-mitotic neural progenitor cell types involved in neocortex development, for a given species, e.g. neuroepithelial stem cells, apical and basal radial glial and intermediate progenitors [11, 14, 29, 30]. Although the cells do not act the same, there is not enough quantitative data to accurately model each sub-population, thus, P is treated as an aggregate compound population.

The neuron population is, similarly, a compound population encompassing all post-mitotic and permanently differentiated neurons. Note that we are only interested in population dynamics local to the cortex and, as such, exclude movement and subsequent spatial information. Critically, neuron migration does occur, which is explicitly included in our model in terms of the final scaling of the data

rather than as a physical movement term (discussed later) [31, 32].

The division rate of a progenitor, ρ, is the same, no matter the resulting outcome. However, the transitions are not equally likely. As such, we introduce, three probabilities α, ν and σ, such that $1 = \alpha + \nu + \sigma$. From this we define: α to be the probability that the D_a transition takes place; ν to be the probability that the D_n transition takes place; and, finally, $\sigma = 1 - \alpha - \nu$ to be the probability that the D_s transition takes place.

We note that the coordinate triple, (α, ν, σ), defines a ternary coordinate system. Specifically, the coordinate triple is valid if and only if it exists in the space defined in Figure 2, which we will call the strategy space. Namely, the focus of this paper is to determine how the probabilities must evolve in this ternary space in order to specify a developing cortex. Figure 2 illustrates a potential dotted trajectory.

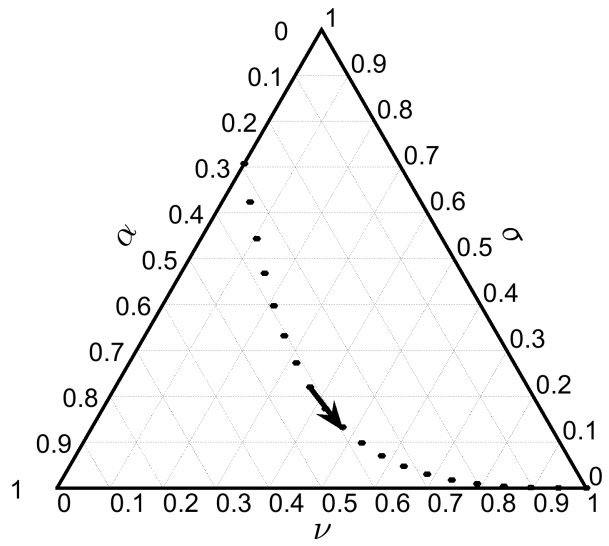

Figure 2: Illustration of the ternary coordinate system that will be used to define the strategy space. The curved, dotted line and arrow illustrates the evolution of the transition probabilities. Initially, the probabilities of symmetric and asymmetric transition are $\sigma = 0.7$ and $\alpha = 0.3$, respectively. As the strategy evolves σ decreases, whilst α and ν increase. Finally, α and σ decrease to zero whilst $\nu \to 1$.

From these definitions the resulting set of ODEs defining this system is, thus,

$$\frac{\mathrm{d}P}{\mathrm{d}t} = \rho P\left(1 - \alpha - 2\nu\right), \quad P(t_0) = P_0, \tag{1}$$

$$\frac{\mathrm{d}N}{\mathrm{d}t} = \rho P\left(\alpha + 2\nu\right), \quad N(t_0) = 0, \tag{2}$$

where t_0 is the time of onset of neurogenesis and P_0 is the founder progenitor population. We also fix t_F as the final time of neurogenesis, so equations (1) and (2) are only valid for $t \in [t_0, t_F]$. Due to the linearity of the equations, we non-dimensionalise all populations with respect to the initial progenitor population, *i.e.* $P \mapsto P/P_0$ and $N \mapsto N/P_0$. We abuse notation by keeping P and N as the name of the non-dimensionalied populations as the form of equations (1) and (2) and associated parameters do not change. The only difference is that the initial condition of P is now $P(t_0) = 1$ and, hence, P and N represent multiples of the initial progenitor population. Although we discuss both dimensional and dimensionless forms of the populations we will explicitly clarify which one is being considered, to remove any ambiguity.

If α and ν are constant then due to this system being linear, the resulting solution is a trivial superposition of exponential functions. Thus, apart from finely tuned marginal cases, where progenitor

populations are constant, the progenitor population must either exponentially increase, or decrease. Since neither case is realistic [12] we extend each transition probability to be time dependent, namely $(\alpha, \nu, \sigma) \mapsto (\alpha(t), \nu(t), \sigma(t))$. Specifically, D_s is preferred early in neurogenesis in order to rapidly create a viable population of progenitors and, hence, consequently, neurons. During neurogenesis the probability of D_a increases to a peak before both D_s and D_a decrease leaving D_n as the dominant preferred mode of division during late neurogenesis (see Figure 2).

For simplicity, we define the probabilities to be piecewise functions, namely

$$\alpha(t) = \begin{cases} \alpha_0 + \frac{\alpha_S - \alpha_0}{t_S - t_0}(t - t_0) & t \in [t_0, t_S], \\ \alpha_S \left(1 - \frac{t - t_S}{t_F - t_S}\right) & t \in (t_S, t_F], \end{cases} \tag{3}$$

$$\nu(t) = \begin{cases} 0 & t \in [t_0, t_S], \\ \nu_F \left(\frac{t - t_S}{t_F - t_S}\right) & t \in (t_S, t_F], \end{cases} \tag{4}$$

and $\sigma(t) = 1 - \alpha(t) - \nu(t)$ as before. This introduces four new parameters: t_S, the strategy switching time; α_0 the initial probability of D_a; α_S, the probability of D_s at $t = t_S$; and ν_F the probability of D_n at $t = t_F$ (see Figure 3). The time t_S distinguishes two phases of the neurogenic process. Initially D_a is increasingly preferred over D_s. In a second phase D_n is introduced and gradually takes on as the most abundant mode of division. By constraining the parameters to satisfy

$$0 \leq \alpha_0 < \alpha_S \leq 1, \quad 0 < \nu_F \leq 1, \quad t_0 < t_S < t_F, \tag{5}$$

then the four parameters always define a valid trajectory in strategy space.

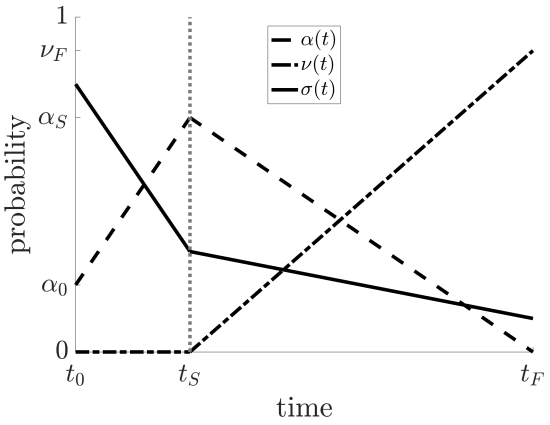

Figure 3: Illustrating the temporal piecewise definitions of (α, ν, σ) and their dependence on the variables $(t_S, \alpha_0, \alpha_S, \nu_F)$.

Similarly, although we initially consider ρ to be constant, we will later add a temporal dimension to this variable to account for the experimentally observed modulation of the cell cycle length throughout the course of neurogenesis [33]. Specifically, cell cycle length, T_c, and ρ are related through

$$\rho(t) = \log\left(\frac{2}{T_c(t)}\right). \tag{6}$$

As above, we define $T_c(t)$ to be piecewise linear in time, using data on mouse, macaque and human to interpolate and specify the gradients and intercepts [34].

It should be noted that a posteriori checks of the piecewise linear assumptions were made (data not shown). Critically, using smooth functions instead of piecewise definitions did not change the

qualitative results and hardly changed the quantitative fitting results. Thus, the piecewise linear definitions provide a simple, robust and minimalist way of closing the system.

Finally, we notice that equation (2) does not contain a natural decay term for the neuron population. Equally, the influence of migration are ignored. Surprisingly, these two effects nearly cancel each other out. Indeed, post-neurogenesis, it is estimated that there is a bulk loss of 30% of adult cortical neurons and a net increase of 25% through interneurons migrating to the cortex [35–38]. Thus, these bulk population corrections are accounted for when integrating experimental estimates of final neurogenic output into the model. Specifically, if $\bar{N}$ is the experimentally derived estimate for final neuron number then the dimensional size of N, as derived from equations (1) and (2), is

$$N(t_F) = \bar{N}(1+\delta)(1-\mu), \tag{7}$$

where δ is the proportion of neurons lost to apoptosis (here, $\delta = 0.3$) and μ is the proportion gained by migration (here, $\mu = 0.25$). Later we show that the results are robust to variations in these quantities.

3 Data fitting

Our study will focus on three mammalian species: mouse, macaque monkey, and human (Figure 4). Although data on other mammalian species exist, we focus on these three, as previous studies have chosen them to effectively illustrate neocortex development across distinct branches of the phylogenetic tree [11].

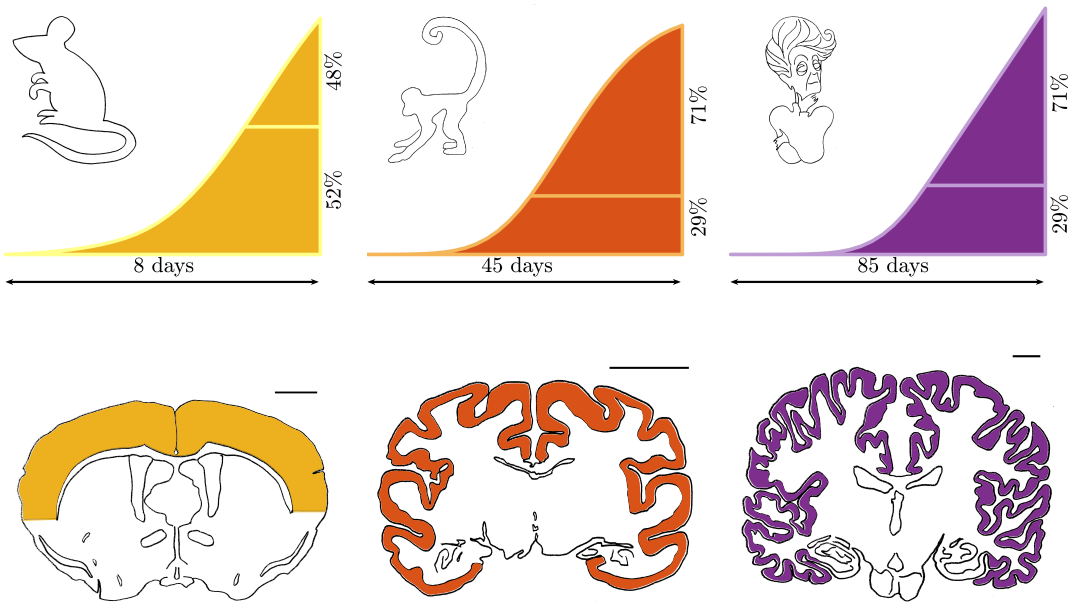

Figure 4: Cortical development in mouse, macaque monkey, and human. Top row: the timing of production and proportions of these neurons residing in deeper and upper layers vary in each species. Upper layer neuron production starts at t_M : E17 in mouse, E64 in monkey, E93 in human (where E indicates embryonic day), producing a different ratio of deeper layer neurons φ : 0.52 in mouse, 0.29 in monkey and human. Bottom row: coronal brain cross sections highlight the progressive increase in size and convolution of the cerebral cortex (coloured region). Scale bars indicate 1 mm, 10 mm and 10 mm, respectively. Data from [39, 40].

Neural progenitors are initially positioned along the apical (inner) surface of the developing brain,

with processes (protrusion of their cell body) extending to the pial (outer) surface. At birth neurons move along these processes, past pre-existing neurons, to the outermost position. This "inside-first, outside-last" order will eventually result in a six-layered organisation, typical of a mammalian cortex [41]. Hence, time of birth, laminar position, and fate of a neuron, are tightly related. Initially, we fit our non-dimensionalised model to the observed time-dependent production of the cortical layers.

We do a simple parameter search of the strategy space (possible due to its low dimension) to find the strategy, or strategies, which provide the best match for experimental data. Specifically, observations suggest that, to a first approximation, half of the total neurogenic output in mouse is produced in the first half of neurogenesis and the remainder in the second half [42]. This ratio is different in primates, where the second half of neurogenesis is characterised by an increased neuronal production. The result is a significant expansion of the supergranular (upper) layers with respect to the infragranular (deeper) layers [39] (see Figure 4, top row). Thus, we try to find strategies that best approximate

$$N(t_M) = \varphi N(t_F), \tag{8}$$

where φ is the species-specific ratio of neurons in deeper layers, and t_M is the midpoint of neurogenesis, defined as the time when production of deeper layer neurons is completed and production of upper layer neurons starts. Of course, an exact match is highly unlikely, thus, we seek to minimise

$$\epsilon = \left| N(t_F) - \frac{N(t_M)}{\varphi} \right|. \tag{9}$$

The chosen strategy is then extended to encompass the rodent- or primate-specific data by applying a different data derived cell cycle length, T_c, either as a constant or as a time dependent function.

Having parameterised the non-dimensionalised models we seek to estimate the founder populations, P_0, using approximate Bayesian computation (ABC). Specifically, we use an ABC rejection algorithm, which allows us to build a discrete approximation of the posterior distribution of P_0, [43]. The ABC algorithm iteratively draws a proposed value from a uniform prior on some defined region. If the dimensional model, simulated with the proposed P_0, falls close to the data (within a set tolerance) then the value is accepted, otherwise it is rejected. Critically, the tolerance is iteratively updated to ensure that 0.02% of all parameter trials are accepted. The resulting collection of accepted values constitutes an approximation of the posterior distribution, which provides an estimate and error bounds for P_0. Here the fit is run to match one data point, $N(t_F)$.

4 Results

4.1 Mapping species-specific developmental strategies

Frequency of cell cycling is a major determinant of neurogenic output. However, experimental quantification of cell cycle length of human neuronal progenitors is currently unavailable. On the other hand, cell cycle dynamics have been better characterised in mouse and macaque monkey, revealing a different age-dependent variation of the cell cycle length. The mouse progenitors show a steady cell cycle length increase during the course of neurogenesis. In the macaque progenitors, a similar initial trend is then reversed around mid-neurogenesis, resulting in an accelerated rate of late divisions [34]. Given the sparse evidence of cell cycle dynamics in our species of interest, we adopt two alternative representations, constant and age-dependent model, and analyse our results in the light of these two hypotheses. In both representations, the human progenitors are assumed to mirror the macaque cell cycle dynamics at corresponding stages of the neurogenesis window (Figure 5).

The species-specific strategies predicted for the constant and age-dependent cell cycle models are shown in Figure 6. Our estimates reveal that in the first phase, macaque and human favour the prevalence of D_a over D_s considerably more than the mouse (i.e. α_S is larger). This prediction is valid in both cell cycle models. In the second phase a rebound of D_s is predicted for macaque and human (i.e. $\nu_F < \alpha_S$) in the case of the constant cell cycle model, but only for human in the case

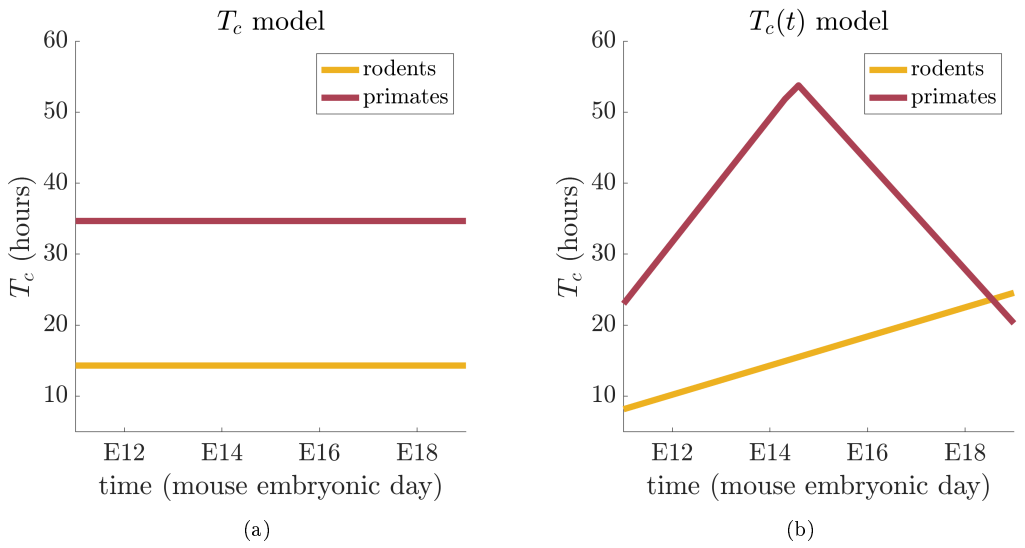

Figure 5: Cell cycle length over different species assuming (a) a constant length and (b) an age-dependent length. Order-specific cell cycle models are parameterized from mouse and macaque monkey data. Mouse progenitor cell cycle duration is: 10.2 hours at E12; 18.4 hours at E16 (data from [12]). Rhesus macaque progenitor cell cycle duration is: 23 hours at E40; 54 hours at E60; 27 hours at E80 (data from [34]). Averages are used for the constant cell cycle models. To facilitate direct comparison, times are converted in equivalent mouse embryonic days (E).

of the age-dependent cell cycle model. Finally, the constant cell cycle model predicts a relative delay in the strategy switching time for increasingly larger species (Figure 6(a)). The prolonged preference for self amplifying divisions is consistent with the need of a larger progenitor pool to allow expansion of supergranular layers produced in the later phases of neurogenesis. In the age-dependent cell cycle model the demand for this expansion in primates is met by the acceleration of cell cycling, and does not result in a delay in the switching time.

Since the developmental strategies are predicted on the non-dimensional system, they are valid for different absolute values of neuronal production, interneuronal migration, or post-neurogenesis cell death. Having calibrated the species- and cell-cycle- specific strategies, we turn to the dimensional model to estimate the initial conditions that match the final neurogenic output, in terms of absolute cell numbers.

4.2 The founder population does not necessarily scale with neurogenic output

The number of progenitor cells present at the onset of neurogenesis is unknown. Experimental measurements are limited to the size of the developing cortex which, at this stage, is almost exclusively occupied by progenitor cells [26, 40]. However, spatial heterogeneity, and cross-species variation in cell size and density makes it impossible to estimate cell numbers for this founder population. We therefore use the model, calibrated to the species-specific developmental strategy, to estimate this number. The model prediction is that the size of the founder population for species of increasingly larger brain size, does not necessarily scale accordingly. Posteriors for P_0 estimates are shown as 'violin' plots in Figure 7 (see dashed gray line), where the vertical width of each distribution represents the support of the posterior, whilst the horizontal width of each distribution represents the density of the posterior. Finally, the horizontal black line across each distribution represents the point estimate giving the best fit to $N(t_F)$. Critically, for both cell cycle models, the estimated human P_0 is unexpectedly lower than

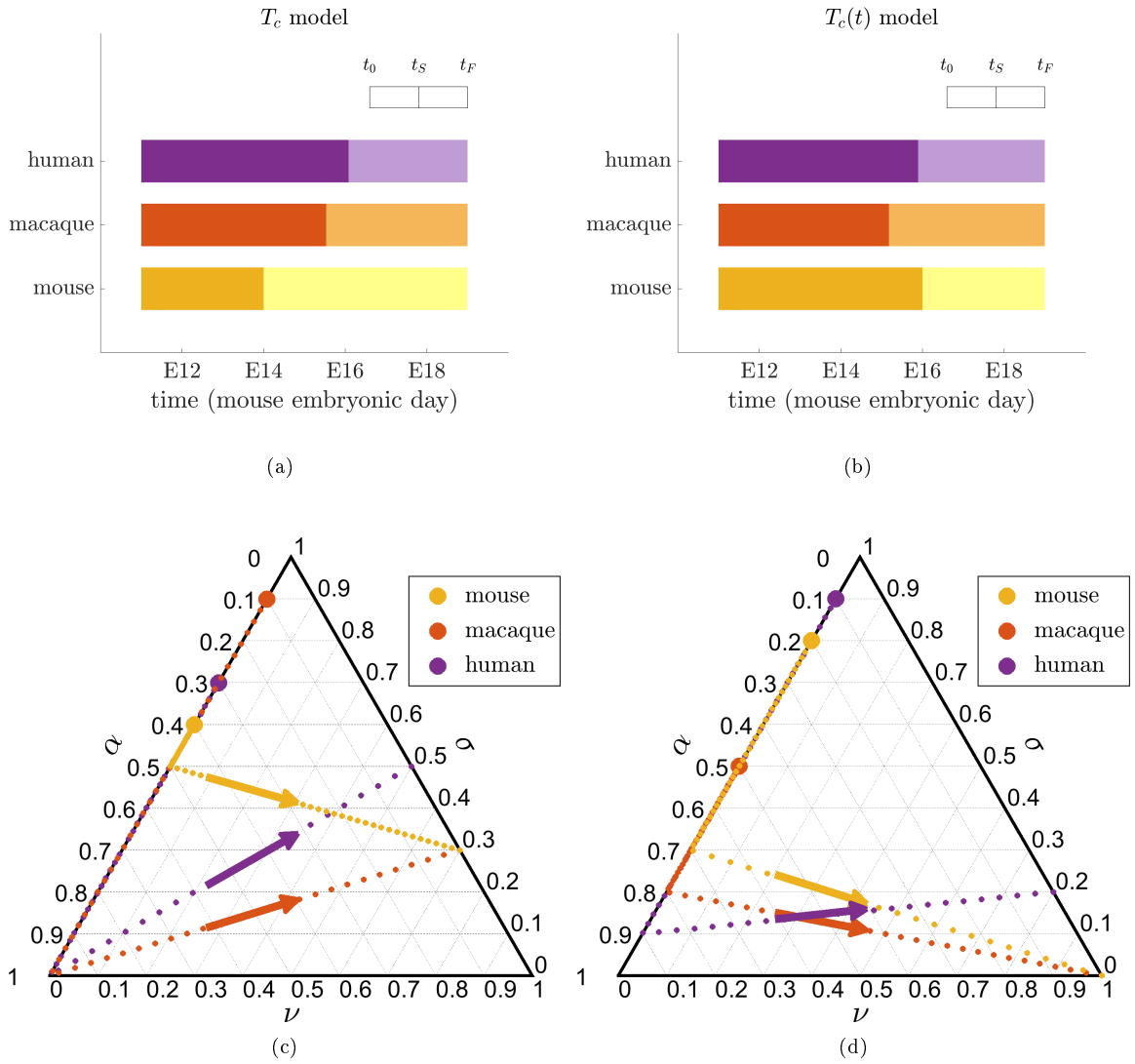

Figure 6: Left column: constant cell cycle model. Right column: age-dependent cell cycle model. (a-b) Species- and cell-cycle-model- specific estimates of the time of switch t_S, represented in equivalent mouse embryonic days. (c-d) Evolution of the transition probabilities in the strategy space. Illustrated strategies are species- and cell-cycle-model- specific estimates. The arrows provide the direction of the trajectory and the big point on the α axis is the initial condition.

both mouse and macaque. Following an allometric scaling argument we would have expected the size of the founder population in humans, to be larger than the macaque and mouse.

4.3 Changes in human progenitor cell cycle length can justify P_0 increase

In order to address this counterintuitive prediction, we challenge the key modelling assumption that could have led us to underestimate the human founder population. The lack of human-specific data required us to introduce the key assumption that the cell cycle is the same in all primates. While in the absence of evidence for the contrary it is sensible to assume that the change in monotonicity of the cell cycle is species-dependent (monotonically increasing in rodents; increasing then decreasing for

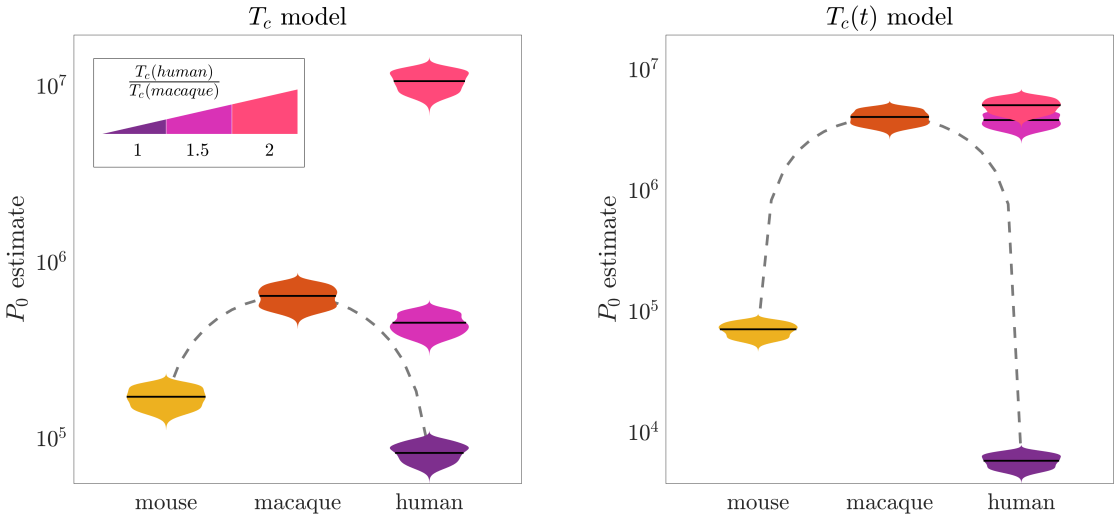

Figure 7: Approximated posterior distributions of species- and cell-cycle-model- specific estimated founder population. Violin plots show symmetric probability density functions of parameter values (y-axis), across species (x-axis). The width of the plot specifies the probability density of providing a given estimate for P_0. Thus, the wider the plot is at a given value on the y-axis the more likely the given value is to be chosen as the estimate. The horizontal black line indicates the P_0 point estimate (best fit). The dashed gray line indicates the predictions based on the current assumption (cell cycle length is conserved across primates). Distributions corresponding to assumption of an amplified T_c (cell cycle length) in human are also shown (see legend).

primates), there is evidence that cells in larger species cycle more slowly [44]. Since no quantitative data on the expansion of the cell cycle in human progenitor cells compared to the macaque is available, we repeat the ABC estimates for representative values of cell cycle amplification in human progenitors, with respect to the baseline macaque values. The additional posteriors for the human P_0 in Figure 7 correspond to amplifications of 1.5 and 2 fold. We find that in both cell cycle models, the estimated founder population scales with the size of the species, when we assume a 2 fold amplification of the human progenitor cell cycle length.

It is worth noting that we used a two-step model calibration. We initially searched the strategy space to capture the qualitative temporal pattern of neurogenic output in the non-dimensional model, specified by the dataset (t_M, φ). The chosen strategy accounts for species-specific factors: duration of neurogenesis, distribution of time of birth and laminar position of neurons, and cell cycle dynamics. However, having used the non-dimensional system, it does not depend on the initial size of the progenitor population. We then estimated the founder population P_0 to quantitatively match the absolute value of neurogenic output, corresponding to the dataset $\left(\bar{N}, \delta, \mu\right)$. Indeed, given the linearity of the system, changes in the rate of post-neurogenesis death and interneuronal migration, will only offset the P_0 estimate, and will not affect the estimated strategy (see equations (7) and (8)).

Finally, we note that the P_0 estimate for the age-dependent cell cycle model changes considerably when going from the baseline to the 1.5 fold amplification, but not as much to the 2 fold amplification (see Figure 7). An intuitive explanation of this result can be given as follows. The predicted P_0 will mostly depend on the number of progenitor self-amplifying divisions happening before t_S. Afterwards most divisions will be neurogenic. The predicted time of switch for the 1.5 and 2 fold amplifications is t_S = E84.5 and t_S = E56, after and before the change in monotonicity of the cell cycle length, respectively (see Figure 8). Hence, the 2 fold amplification strategy reduces production of progenitors

earlier, in the phase where divisions are less frequent. The 1.5 amplification strategy switches at a later stage where divisions are speeding up. However, at these stages the cell cycle length is approximately the same. For the baseline strategy the predicted time of switch is at t_S = E90, when cells are cycling almost twice as fast. Given this enhanced amplification of the P population in the baseline case, the founder population that matches the neurogenic output result is considerably smaller.

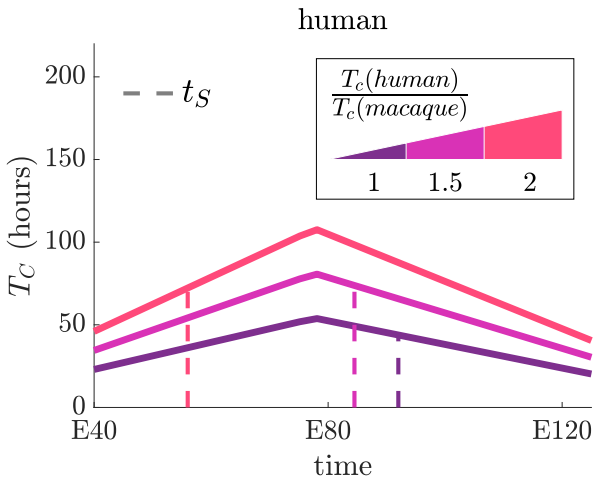

Figure 8: Age-dependent cell cycle length model for human progenitors. Amplifications are colour coded as in Figure 7. Vertical dashed lines indicate the time of switch t_S of the developmental strategy predicted for the given amplification.

4.4 Timing of strategy switch is key

We are interested in testing the robustness of the model to small variations of the estimated developmental strategies. Local sensitivity analysis links the variation of model output y, to variations in the parameter θ:

$$S = \left| \frac{(y - y^*)/y^*}{(\theta - \theta^*)/\theta^*} \right|, \tag{10}$$

where the asterisks denote the values of the parameter and solution at the fitted point.

Here the output of interest is the timely distribution of neurons between deeper and upper layers according to (8):

$$y = \left| N(t_F) - \frac{N(t_F)}{\varphi} \right|. \tag{11}$$

and S is calculated for each one of the model parameters $(\alpha_0, \alpha_S, \nu_F, t_S)$. Across species- and cell-cycle-model- specific strategies, we consistently find the highest sensitivity to variations in the time of strategy switch t_S, and lower sensitivities to variations in the absolute prevalence of different types of divisions α_0, α_S, and ν_F. A representative example of local sensitivity (for the constant cell cycle mouse strategy) is shown in Figure 9.

4.5 Analytical conditions on an expanding-then-shrinking proliferative zone

Experimental observations have consistently found that an initial expansion of the proliferating region occupied by neural progenitors is followed by a progressive shrinkage [34]. As previously noted, if α and ν are constant, the model would not be able to capture such time-dependent behaviour. We ask under which parameter conditions can our time-dependent transition probabilities capture the non-monotonic behaviour expected of the progenitor population, P. Restricting the analysis to a defined

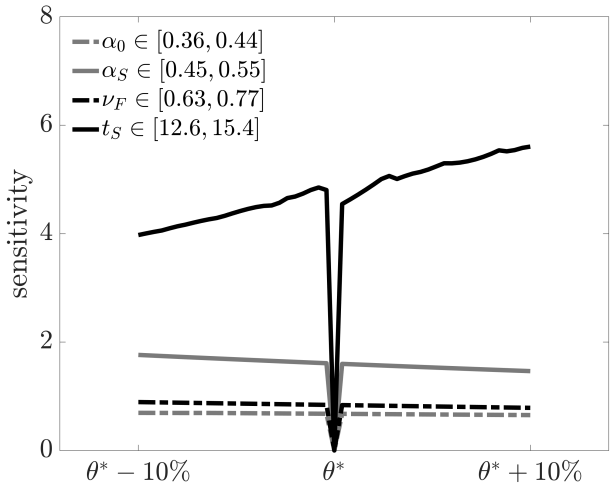

Figure 9: Parameter sensitivity for mouse strategy with constant cell cycle. θ^* indicates the reference value for the corresponding parameter in the predicted strategy. Variations in the $\pm 10\%$ range are considered.

region of the four-dimensional parameter space satisfying equation (5), it is possible to find a sufficient condition for non-monotonicity.

Lemma 4.1 *If* $1/2 < \nu_F < 1$ *then* $P(t)$ *attains a maximum at* $t^* \in (t_S, t_F)$, *where*

$$t^* = t_S + \frac{\alpha_S - 1}{\alpha_S - 2\nu_F} (t_F - t_S) . \tag{12}$$

In all other parameter regimes, $P(t)$ *is monotonically increasing for all* $t \in [t_0, t_F]$.

Coincidentally, the estimated strategies all are within this region. This means that the strategy predicted mathematically, by fitting the very limited temporal data available, is also biologically realistic. Figure 10 shows the temporal evolution of the progenitor and neuronal populations in the mouse, macaque and human neurogenesis models. In all species and both cell cycle models the progenitor population follows the expected qualitative behaviour, recapitulating the expansion followed by shrinkage of the proliferating region of the developing cortex.

An additional model prediction which finds support in the biology is that at the end of neurogenesis there is a remaining non-depleted progenitor population, i.e. $P(t_F) \gg 0$. Consecutive to the time window of our interest is a gliogenic period, when the remaining progenitor population, following a process similar to the neurogenic one, terminally differentiates in glia cells. Glia cells, including astrocytes and oligodendrocytes, are essential for the maintenance of homeostasis, and are present in the adult brain in numbers comparable to the neurons. Essential to their correct formation is the presence of a non-depleted progenitor population at the onset of gliogenesis [45], which our model reproduces.

5 Discussion

A complete biological system spans many temporal scales, from the diffusion of proteins across membranes taking microseconds to the age related transitions of hair colour taking decades (see Figure 11). Of course, when investigating a single phenomenon many of these time scales will decouple through

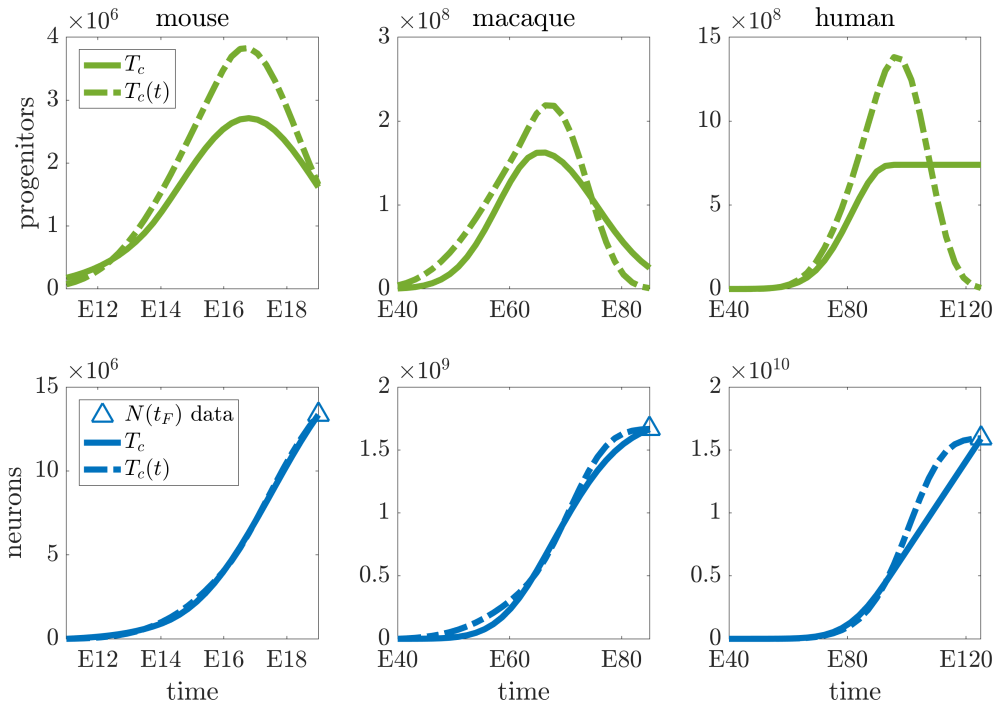

Figure 10: Population dynamics resulting from different species- and cell-cycle-model- specific developmental programmes.

the use of quasi-steady state assumptions, such that phenomena on faster time scales are always in equilibrium within the current system state, whilst activities on slower time scales effectively do not change over the time period of interest [46].

Figure 11: A visual example of biological time scales and their influence on hair colour. Left to right: author Dr Thomas E. Woolley, Prof. Philip K. Maini and Prof. Jim D. Murray.

Here, we have considered the development of the mammalian cerebral neocortex, in which temporal changes in cellular division strategy cannot be ignored. Namely, neural progenitor cells initially tend to reproduce themselves through symmetric and asymmetric division, whilst later in development they produce terminally differentiated neurons.

Despite the limited resolution of the experimental data currently available, we could recapitulate the key temporal dynamics of cortical neurogenesis. Starting from a limited set of representative species, we aimed at shedding light on the evolution of the mammalian cortex, by means of branching from

a communal developmental process. In drawing conclusions regarding such divergent mechanisms, we are highly constrained by the lack of experimental quantification.

We highlighted the drawbacks in introducing a priori scaling assumptions on unknown quantities such as the size of the founder population and the cell cycle length. Carrying out experimental quantifications in brains of larger species, in particular the human, is challenging, costly, time-consuming and at times limited by ethical considerations. As a result, the biological community studying cortical development often adopts simplifying assumptions, invoking order-specific similarities (e.g. assuming that all primates have similar cell cycle dynamics) or a priori scaling rules (e.g. extrapolating the relative increase in cell cycle length between mouse and macaque, deducing an even larger cell cycle length in human progenitors). Since we intend to build a model that can mechanistically explain the cross-species variation, we do not simply adopt scaling rules, but consider different levels of amplification of the cell cycle length of human progenitors with respect to the macaque baseline. We then determine the effects of different levels of such amplification on the predicted size of the founder population. The high variation in the model prediction highlights the need to focus experimental resources on the quantification of cell cycle dynamics in human progenitors. Conversely sensitivity analysis suggests that relative proportions of division modes are not as important as the switching time. The latter could be important for developmental disorders, often associated with a mistimed switch between proliferative and differentiative divisions. An example is primary microcephaly, characterised by centrosomal abnormalities that affect mitosis and cell fate specification [47].

Further, although constrained by the lack of data, mathematical modelling has provided a number of key insights that either clarify mechanisms, or direct future experimentation. For example, the sensitivity analysis has allowed us to pinpoint exactly the parameters that need to be finely tuned and, thus, accurately derived from experimental observations. For the reader interested in understanding the influence of perturbations to these finely tuned parameters we offer the neurogenesis simulator, which can be used to quickly and easily calculate the outcomes as model parameters and assumptions are varied.

Finally, we must question the reality of our result that humans have lower founder progenitor populations when compared to macaques. Currently, this result fits all experimental insights provided by neurobiological colleagues [Pers. Comms, see acknowledgements] and accounts for all known data [11, 12, 15, 16, 33, 34, 48, 49]. Moreover, there are evolutionary arguments in favour of this result. Namely, our results regarding progenitor populations suggests that the developmental variations of different species simply arise from using the same conserved raw biological materials under different strategies, rather than demanding a different set, or amount of, raw materials for each species. Conversely, if the neurogenic output correlated to founder population size then brains of larger animals would be prohibitively large and not possible to produce.

In the future we intend to use our strategy space as means of mapping evolutionary trajectories that describe neurogenesis in different species. Further, we aim to use deviations from such strategies as a means of diagnosing brain diseases that appear when the developmental program goes awry.

6 Acknowledgements

NP was supported from a St John's College Research Centre Grant to TEW, Philip K. Maini and Zoltán Molnár in collaboration with Fernando García-Moreno.

References

[1] A. M. Turing. The chemical basis of morphogenesis. *Phil. Trans. R. Soc. Lond. B*, 237:37–72, 1952.

[2] A. Gevins and M. E. Smith. Detecting transient cognitive impairment with eeg pattern recognition methods. *Aviat. Space Environ. Med.*, 70(10):1018–1024, 1999.

[3] S. C. van der Linde, T. A. Nijhuis, F. H. M. Dekker, F. Kapteijn, and J. A. Moulijn. Mathematical treatment of transient kinetic data: Combination of parameter estimation with solving the related partial differential equations. *Appl. Catal., A*, 151(1):27–57, 1997.

[4] C. C. Pantelides, D. Gritsis, K. R. Morison, and R. W. H. Sargent. The mathematical modelling of transient systems using differential-algebraic equations. *Comp. chem. engin.*, 12(5):449–454, 1988.

[5] O. Schein and G. Denk. Numerical solution of stochastic differential-algebraic equations with applications to transient noise simulation of microelectronic circuits. *J. Comput. Appl. Math.*, 100(1):77–92, 1998.

[6] L. J. Schumacher, T. E. Woolley, and R. E. Baker. Noise-induced temporal dynamics in turing systems. *Phys. Rev. E*, 87(4):042719, 2013.

[7] J. L. Aragón, R. A. Barrio, T. E. Woolley, R. E. Baker, and P. K. Maini. Nonlinear effects on turing patterns: Time oscillations and chaos. *Phys. Rev. E*, 86(2):026201, 2012.

[8] T. E. Woolley, R. E. Baker, E. A. Gaffney, P. K. Maini, and S. Seirin-Lee. Effects of intrinsic stochasticity on delayed reaction-diffusion patterning systems. *Phys. Rev. E*, 85(5):051914, 2012.

[9] J. M. Fuster. The prefrontal cortex—an update: time is of the essence. *Neuron*, 30(2):319–333, 2001.

[10] C. G. Woods. Human microcephaly. *Curr. Opin. Neurobiol.*, 14(1):112–117, 2004.

[11] P. Rakic. A small step for the cell, a giant leap for mankind: a hypothesis of neocortical expansion during evolution. *Trends Neurosci.*, 18(9):383–388, 1995.

[12] T Takahashi, R. S. Nowakowski, and V. S. Caviness. The leaving or q fraction of the murine cerebral proliferative epithelium: a general model of neocortical neuronogenesis. *J. Neurosci.*, 16 (19):6183–6196, 1996.

[13] I. Imayoshi and R. Kageyama. bhlh factors in self-renewal, multipotency, and fate choice of neural progenitor cells. *Neuron*, 82(1):9–23, 2014.

[14] M. Florio and W. B. Huttner. Neural progenitors, neurogenesis and the evolution of the neocortex. *Development*, 141(11):2182–2194, 2014.

[15] P. Rakic. Specification of cerebral cortical areas. *Science*, 241(4862):170, 1988.

[16] S. Herculano-Houzel. The remarkable, yet not extraordinary, human brain as a scaled-up primate brain and its associated cost. *Proc. Nat. Acad. Sci.*, 109(Supplement 1):10661–10668, 2012.

[17] B. Mota and S. Herculano-Houzel. Cortical folding scales universally with surface area and thickness, not number of neurons. *Science*, 349(6243):74–77, 2015.

[18] M. C. Weis, J. Avva, J. W. Jacobberger, and S. N. Sreenath. A data-driven, mathematical model of mammalian cell cycle regulation. *PloS one*, 9(5):e97130, 2014.

[19] B. Novak and J. J. Tyson. Numerical analysis of a comprehensive model of m-phase control in xenopus oocyte extracts and intact embryos. *J. Cell Sci.*, 106(4):1153–1168, 1993.

[20] L. Calzone, D. Thieffry, J. J. Tyson, and B. Novak. Dynamical modeling of syncytial mitotic cycles in drosophila embryos. *Mol. Syst. Biol.*, 3(1):131, 2007.

[21] M. Sturrock, A. Hellander, A. Matzavinos, and M. A. J. Chaplain. Spatial stochastic modelling of the hes1 gene regulatory network: intrinsic noise can explain heterogeneity in embryonic stem cell differentiation. *J. Roy. Soc. Interface*, 10(80):20120988, 2013.

[22] C. T. H. Baker, G. A. Bocharov, and C. A. H. Paul. Mathematical modelling of the interleukin-2 t-cell system: A comparative study of approaches based on ordinary and delay differential equation. *Comput. Math. Methods Med.*, 1(2):117–128, 1997.

[23] R. Thomas and M. Kaufman. Multistationarity, the basis of cell differentiation and memory. ii. logical analysis of regulatory networks in terms of feedback circuits. *Chaos*, 11(1):180–195, 2001.

[24] K. L. Spalding, O. Bergmann, K. Alkass, S. Bernard, M. Salehpour, H. B. Huttner, E. Boström, I. Westerlund, C. Vial, B. A. Buchholz, G. Possnert, D. C. Mash, H. Druid, and J. Frisén. Dynamics of hippocampal neurogenesis in adult humans. *Cell*, 153(6):1219–1227, 2013.

[25] F. Ziebell, A. Martin-Villalba, and A. Marciniak-Czochra. Mathematical modelling of adult hippocampal neurogenesis: effects of altered stem cell dynamics on cell counts and bromodeoxyuridine-labelled cells. *J. Roy. Soc. Interface*, 11(94):20140144, 2014.

[26] E. Lewitus, I. Kelava, A. T. Kalinka, P. Tomancak, and W. B. Huttner. An adaptive threshold in mammalian neocortical evolution. *PLoS Biol.*, 12(11):e1002000, 2014.

[27] S. R. Leffler, E. Legué, O. Aristizábal, A. L. Joyner, C. S. Peskin, and D. H. Turnbull. A mathematical model of granule cell generation during mouse cerebellum development. *Bull. Math. Biol.*, 78(5):859–878, 2016. doi: 10.1007/s11538-016-0163-3.

[28] N. Picco, F. García-Moreno, P. K. Maini, T. E. Woolley, and Z. Molnár. Mathematical modeling of cortical neurogenesis reveals that the founder population does not necessarily scale with neurogenic output. *Cereb. Cortex*, 28(7):2540–2550, 2018.

[29] W. B. Huttner and M. Brand. Asymmetric division and polarity of neuroepithelial cells. *Curr. Opin. Neurobiol.*, 7(1):29–39, 1997.

[30] S. C. Noctor, V. Martínez-Cerdeño, L. Ivic, and A. R. Kriegstein. Cortical neurons arise in symmetric and asymmetric division zones and migrate through specific phases. *Nat. Neurosci.*, 7 (2):136–144, 2004.

[31] M. Barber and A. Pierani. Tangential migration of glutamatergic neurons and cortical patterning during development: Lessons from cajal-retzius cells. *Dev. neurobiol.*, 76(8):847–881, 2016.

[32] F. García-Moreno, E. Anderton, M. Jankowska, J. Begbie, J. M. Encinas, M. Irimia, and Z. Molnár. Absence of tangentially migrating glutamatergic neurons in the developing avian brain. *Cell reports*, 22(1):96–109, 2018.

[33] C. Dehay and H. Kennedy. Cell-cycle control and cortical development. *Nat. Rev. Neurosci.*, 8 (6):438–450, 2007.

[34] D. R. Kornack and P. Rakic. Changes in cell-cycle kinetics during the development and evolution of primate neocortex. *Proc. Nat. Acad. Sci.*, 95(3):1242–1246, 1998.

[35] F. García-Moreno, L. López-Mascaraque, and J. A. De Carlos. Origins and migratory routes of murine cajal-retzius cells. *J. Comp. Neurol.*, 500(3):419–432, 2007.

[36] M. Pompeiano, A. J. Blaschke, R. A. Flavell, A. Srinivasan, and J. Chun. Decreased apoptosis in proliferative and postmitotic regions of the caspase 3-deficient embryonic central nervous system. *J. Comp. Neurol.*, 423(1):1–12, 2000.

[37] C.-Y. Kuan, K. A. Roth, R. A. Flavell, and P. Rakic. Mechanisms of programmed cell death in the developing brain. *Trends Neurosci.*, 23(7):291–297, 2000.

[38] Z. Petanjek, I. Kostovic, and M. Esclapez. Primate-specific origins and migration of cortical gabaergic neurons. *Front. Neuroanat.*, 3:26, 2009.

[39] C. J. Charvet, D. J. Cahalane, and B. L. Finlay. Systematic, cross-cortex variation in neuron numbers in rodents and primates. *Cereb. Cortex*, 25(1):147–160, 2013.

[40] A. D. Workman, C. J. Charvet, B. Clancy, R. B. Darlington, and B. L. Finlay. Modeling transformations of neurodevelopmental sequences across mammalian species. *J. Neurosci.*, 33(17): 7368–7383, 2013.

[41] S. K. McConnell and C. E. Kaznowski. Cell cycle dependence of laminar determination in developing neocortex. *Science*, 254(5029):282–285, 1991.

[42] H. Markram, M. Toledo-Rodriguez, Y. Wang, A. Gupta, G. Silberberg, and C. Wu. Interneurons of the neocortical inhibitory system. *Nat. Rev. Neurosci.*, 5(10):793–807, 2004.

[43] N. Picco, E. Sahai, P. K. Maini, and A. R. A. Anderson. Integrating models to quantify environment-mediated drug resistance. *Cancer Res.*, 77(19):5409–5418, 2017.

[44] S. Maciak and P. Michalak. Cell size and cancer: a new solution to peto's paradox? *Evol. Appl.*, 8(1):2–8, 2015.

[45] A. Mallamaci. Developmental control of cortico-cerebral astrogenesis. *Int. J. Dev. Biol.*, 57(9-10): 689–706, 2013.

[46] J. D. Murray. *Mathematical Biology I: An Introduction*, volume 1. Springer-Verlag, 3rd edition, 2003.

[47] E. C. Gilmore and C. A. Walsh. Genetic causes of microcephaly and lessons for neuronal development. *Wiley Interdiscip. Rev. Dev. Biol.*, 2(4):461–478, 2013.

[48] T. F. Haydar, R. S. Nowakowski, P. J. Yarowsky, and B. K. Krueger. Role of founder cell deficit and delayed neuronogenesis in microencephaly of the trisomy 16 mouse. *J. Neurosci.*, 20(11): 4156–4164, 2000.

[49] F. A. C. Azevedo, L. R. B. Carvalho, L. T. Grinberg, J. M. Farfel, R. E. L. Ferretti, R. E. P. Leite, W. J. Filho, R. Lent, and S. Herculano-Houzel. Equal numbers of neuronal and nonneuronal cells make the human brain an isometrically scaled-up primate brain. *J. Comp. Neurol.*, 513(5): 532–541, 2009.